BNWL-366

3-

AEC RESEARCH and DEVELOPMENT REPORT

THE IRRADIATION BEHAVIOR OF UO_2-PuO_2 FUELS IN PRTR

M. D. FRESHLEY
F. E. PANISKO

MARCH, 1967

BATTELLE-NORTHWEST
BATTELLE MEMORIAL INSTITUTE / PACIFIC NORTHWEST LABORATORY

LEGAL NOTICE

PACIFIC NORTHWEST LABORATORY
RICHLAND, WASHINGTON
operated by
BATTELLE MEMORIAL INSTITUTE
for the
UNITED STATES ATOMIC ENERGY COMMISSION UNDER CONTRACT AT(45-1)-1830

PRINTED BY/FOR THE U. S. ATOMIC ENERGY COMMISSION

AEC-RLOO RICHLAND, WASH.

BNWL-366

UC-25, Metals, Ceramics
and Materials

THE IRRADIATION BEHAVIOR OF UO_2-PuO_2 FUELS IN PRTR

By

M. D. Freshley

F. E. Panisko

Fuels Development Section
Materials Department

March, 1967

PACIFIC NORTHWEST LABORATORY
RICHLAND, WASHINGTON

Printed in the United States of America
Available from
Clearinghouse for Federal Scientific and Technical Information
National Bureau of Standards, U.S. Department of Commerce
Springfield, Virginia 22151
Price: Printed Copy $3.00; Microfiche $0.65

TABLE OF CONTENTS

LIST OF FIGURES iv
INTRODUCTION 1
SUMMARY AND CONCLUSIONS 1
IRRADIATION ALTERATION OF VIBRATIONALLY COMPACTED
UO_2-PuO_2 FUEL 3
MOLTEN FUEL OPERATION 6
DEFECT BEHAVIOR 11
FERTF Test A: 11
FERTF Test B: 11
FERTF Test C: 11
FERTF Test D: 12
FERTF Test E: 12
FERTF Test F: 13
FERTF Test G: 13
FERTF Test H: 14
FISSION PRODUCT MIGRATION 17
FISSION GAS RELEASE 18
ACKNOWLEDGEMENT 21
REFERENCES 21
DISTRIBUTION 23

LIST OF FIGURES

Figure		Page
1	PRTR High Power Density Nineteen-Rod Cluster Fuel Element.	3
2	Transverse Section Through a Vibrationally Compacted UO_2–2 wt% PuO_2 PRTR Fuel Rod Which Operated at a Power Generation of 20 kW/ft to a Burnup of 1350 MWd/tonne with Estimated Maximum Fuel Temperatures of 2600 to 2700 °C.	4
3	Transverse Section Through the Axial Midpoint of a Vibrationally Compacted UO_2–2 wt% PuO_2 PRTR Fuel Rod.	5
4	Photomicrograph of a Transverse Section from an Irradiated PRTR Fuel Rod Containing Vibrationally Compacted, Pneumatically Impacted UO_2–4 wt% PuO_2 Fuel.	6
5	Longitudinal Section of the Bottom End Region of a Vibrationally Compacted UO_2-PuO_2 PRTR Fuel Rod.	8
6	Transverse Sections at Different Planes Along the Length of a Vibrationally Compacted UO_2–4 wt% PuO_2 PRTR Fuel Rod.	9
7	Photomosaic of a Transverse Section Through an Intentionally Defected UO_2–2 wt% PuO_2 PRTR Fuel Rod.	14
8	Transverse Sections Through an Intentionally Defected and a Non-defected Vibrationally Compacted UO_2–2 wt% PuO_2 PRTR Fuel Rod.	15
9	Cladding Rupture in a Vibrationally Compacted UO_2–4 wt% PuO_2 PRTR Fuel Rod.	16
10	Transverse Section from the Upper Portion of the Ruptured Intentionally Defected PRTR Fuel Rod.	16
11	Fission Product and Plutonium Distribution in the Intentionally Defected UO_2–2 wt% PuO_2 PRTR Fuel Rod Shown in Figures 7 and 8.	19
12	Fission Gas Release as a Function of Volumetric Average Fuel Rod Temperature in Vibrationally Compacted UO_2-PuO_2 PRTR Fuel Rods.	20

THE IRRADIATION BEHAVIOR OF UO_2-PuO_2 FUELS IN PRTR

M. D. Freshley and F. E. Panisko

INTRODUCTION

Both government and industry are investigating plutonium recycle in thermal reactors.[1] Indications are that during the period of several years needed to fully develop fast reactors, plutonium recycle in thermal reactors will find commercial use.

The principal AEC program in this field is being conducted at Pacific Northwest Laboratory where one of the more important parts of the Plutonium Utilization Program is fuels development.[2] Plutonium fuels development has been concentrated on design and evaluation of fuel elements that can be fabricated at minimum incremental costs beyond those of equivalent uranium fuels. One of the principal objectives of the fuels program is to investigate the potential of plutonium enriched fuels at operating conditions higher than those currently used in power reactors and to determine if there are behavioral differences between plutonium enriched fuels and equivalent UO_2 fuel.

More than 290 experimental fuel elements[3] have been irradiated in the Plutonium Recycle Test Reactor (PRTR)[4] since startup in July 1961. Maximum burnups as high as 10,000 MWd/tonne have been attained. The program at Pacific Northwest Laboratory has emphasized both swaged and vibrationally compacted UO_2-PuO_2 fuels.

The testing program in PRTR was recently expanded to include an evaluation of the irradiation performance of fuel elements containing vibrationally compacted, pneumatically impacted UO_2-PuO_2 operating at high specific powers.[5,6] Irradiation tests of vibrationally compacted UO_2-PuO_2 High Power Density (HPD)* fuel elements (Figure 1) have been conducted in the PRTR to maximum burnups of 4950 MWd/tonne under the maximum conditions expected during the Batch Core Experiment, i.e., maximum rod power generations of 19 to 20 kW/ft with fuel centerline temperatures near melting. Irradiation tests of both nondefected and intentionally defected UO_2-PuO_2 fuel rods conducted in the Fuel Element Rupture Test Facility (FERTF)[10] at maximum rod powers to 27 kW/ft with significant fuel melting produced significant data.

SUMMARY AND CONCLUSIONS

The irradiation behavior of full-sized, mixed-oxide (UO_2-PuO_2) fuel elements is being investigated under power reactor conditions in the Plutonium Recycle Test Reactor (PRTR) at Pacific Northwest Laboratory to obtain information related to plutonium utilization in thermal reactors.

Vibrationally compacted UO_2-PuO_2 fuel structures change significantly when

---

* *The High Power Density Program (HPD) includes the Batch Core Experiment in PRTR to evaluate the physics parameters of a plutonium enriched fuel loading as a function of burnup under controlled conditions.*[7-9]

irradiated at rod powers of 20 kW/ft with centerline fuel temperatures near melting. These changes are similar to those occurring in other oxide fuels irradiated under these conditions. Changes in spatial position of the fuel within rods during irradiation have not created operating problems but do affect irradiation behavior. The major changes in fuel structure occur rapidly; whereas, time-temperature dependent sintering effects cause the fuel sintering radius to increase with exposure. In-reactor homogenization and solid-solution formation by UO_2 and PuO_2 interdiffusion commences in pneumatically impacted, physically mixed UO_2-PuO_2 fuel at temperatures sufficient to cause sintering.

Fuel melting, as evidenced by the formation of a well-defined region composed of a cellular appearing structure in the thermal center of the rod, commences in vibrationally compacted (86% TD) UO_2–2 wt% PuO_2 fuel rods at 20 to 21 kW/ft under PRTR operating conditions. The results show that the power to produce melting in vibrationally compacted fuel is ∿20% less than for sintered pellet fuel.

Chemical analysis and autoradiography confirm the existence of convective mixing in molten UO_2-PuO_2 fuel. Such mixing tends to homogenize the molten fuel.

Examination of fuel structures formed during irradiation in long continuous vibrationally compacted fuel rods suggests that radial and axial fuel relocation occurs under molten core conditions. Also, fuel structures that are developed vary considerably, even in like rods exposed to nominally the same conditions. Thus, an evaluation of irradiation behavior based upon a few specimens may be subject to considerable error. Axial fuel relocation is not unique with vibrationally compacted fuel since similar behavior has been reported for pellet-containing fuel rods that have operated with fuel melting.

Generally, the defect behavior of packed-particle fuel rods has been excellent. At the lower power generations, there has been no appreciable fuel washout, significant fuel rod deformation, water-logging effects, or serious hydriding of the Zircaloy cladding. A significant difference did exist between the satisfactory behavior of an intentionally defected rod operating under molten core conditions at 24 kW/ft and the rupture of a defected rod operating at 27 kW/ft. In the latter experiment, the UO_2-PuO_2 fuel became oxidized and caused a reduction in the effective thermal conductivity and/or melting point. It is hypothesized that the expansion of the unexpected large amount of molten fuel was the underlying cause of rupture. Such behavior (i.e., fuel oxidation) is an inherent property of the fuel material and is not believed to be necessarily related to the fabrication process. The small plutonium addition (4 wt%) probably has little effect on the oxidation behavior of UO_2. It appears that the severity of failure for this fuel design is considerably worse at 27 kW/ft than would be predicted from the defect havior at 24 kW/ft.

Alpha autoradiographs of UO_2-PuO_2 fuel specimens that operated with fuel melting suggest a difference in plutonium segregation and migration characteristics between defected and nondefected fuel rods. Defected rods show evidence of possible plutonium migration; whereas, no such evidence is indicated in fuel specimens from nondefected rods. Fission product migration during irradiation in vibrationally compacted UO_2-PuO_2 fuels is similar to that observed in irradiated UO_2 fuels.

Fission gas release results show a maximum of 92% Xe + Kr release from rods that operated with volumetric average fuel rod temperatures of ∿2200 °C, produced by a maximum rod power of 27 kW/ft in PRTR

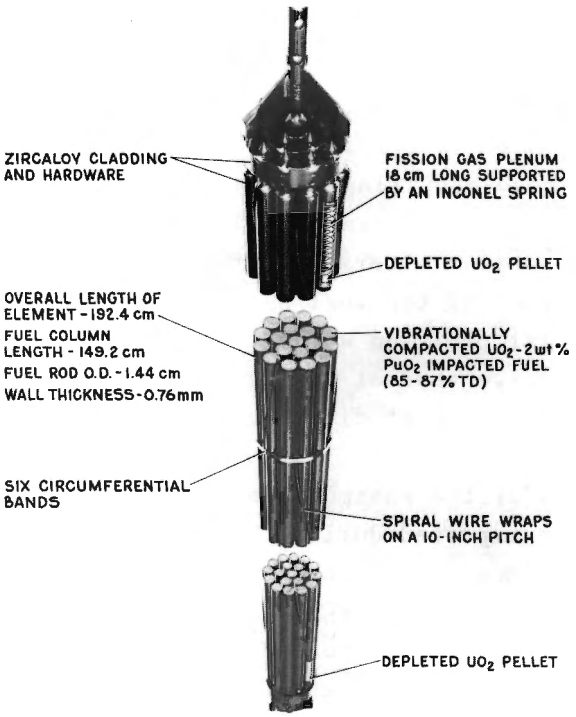

Neg. PNL0661684-2

FIGURE 1. PRTR High Power Density Nineteen-Rod Cluster Fuel Element

IRRADIATION ALTERATION OF VIBRATIONALLY COMPACTED UO_2-PuO_2 FUEL

Pacific Northwest Laboratory has concentrated on the development of vibrationally compacted fuel elements[11] composed of Zircaloy clad rods containing pneumatically impacted UO_2-PuO_2 fuel material (Figure 1). In early particle fuel development work with UO_2 only, arc fusing was employed satisfactorily to produce the high density particles needed to enhance thermal conductivity, fission gas retention, and bulk fuel density in the finished swaged or vibrationally compacted fuel rods. Because arc fusing was not considered feasible for use with plutonium, pneumatic impaction, a closed die, hot forging technique was developed.[12] In this process, the UO_2 and PuO_2 powders, (in appropriate proportions and particle sizes) are mechanically blended prior to impaction. After impaction, the high density oxide (routinely greater than 99% TD) composed of the UO_2-PuO_2 mixture is pulverized and mechanically sieved into different size fractions suitable for either swage or vibrational-compaction. Since pneumatically impacted mixed-oxide fuels consist of discrete UO_2 and PuO_2 particles, the size and distribution of the particles as related to their effect on Doppler response is an important consideration.[13] Pneumatically impacted UO_2-PuO_2 meeting thermal or fast reactor particle size criteria has been prepared by controlling the particle size of the starting materials.[14]

The structure of mixed-oxide fuel changes significantly during irradiation; the degree of alteration depends upon the irradiation conditions and exposure. The changes are similar to those occurring in other ceramic fuel systems during irradiation. Irradiation alteration affects the behavior of the fuel by changing its spatial position within the rod, its effective thermal conductivity, its fission product distribution, and its failure behavior.

Under the maximum operating conditions expected during the Batch Core Experiment, in-reactor sintering and densification of the fuel cause a central void in the thermal center of the rods (Figure 2). A wide band of radially oriented columnar grains surrounds the central void which, in turn, is surrounded by a narrow region of equiaxed grain growth. The columnar grain growth extends to 65% of the radius in the vibrationally compacted UO_2–2 wt% PuO_2 PRTR fuel rod (Figure 2) which was irradiated to a burnup of 1350 MWd/tonne at a maximum rod power of 20 kW/ft. Estimated maximum fuel temperatures were in the range of 2600 to 2700 °C. The equiaxed grain growth region is surrounded by an annulus of structurally unaffected fuel extending to the cladding.

The major changes in fuel structure occur relatively rapidly. Time-temperature dependent sintering effects cause the radius of the sintering boundary to increase with increasing exposure (Figure 3). The columnar grain growth region extends to 85% of the radius in the vibrationally

Photomacrograph

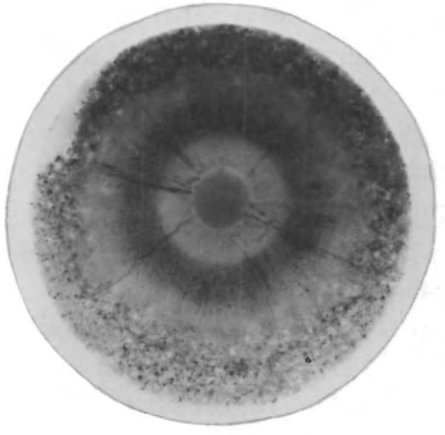

β-γ Autoradiograph

Neg. PNL0661684-3A

3.8X

FIGURE 2. Transverse Section Through a Vibrationally Compacted UO_2–2 wt% PuO_2 PRTR Fuel Rod which Operated at a Power Generation of 20 kW/ft to a Burnup of 1350 MWd/tonne with Estimated Maximum Fuel Temperatures of 2600 to 2700 °C. Columnar Grain Growth Extends to 65% of the Radius. This Represents Maximum Batch Core Experiment Conditions.

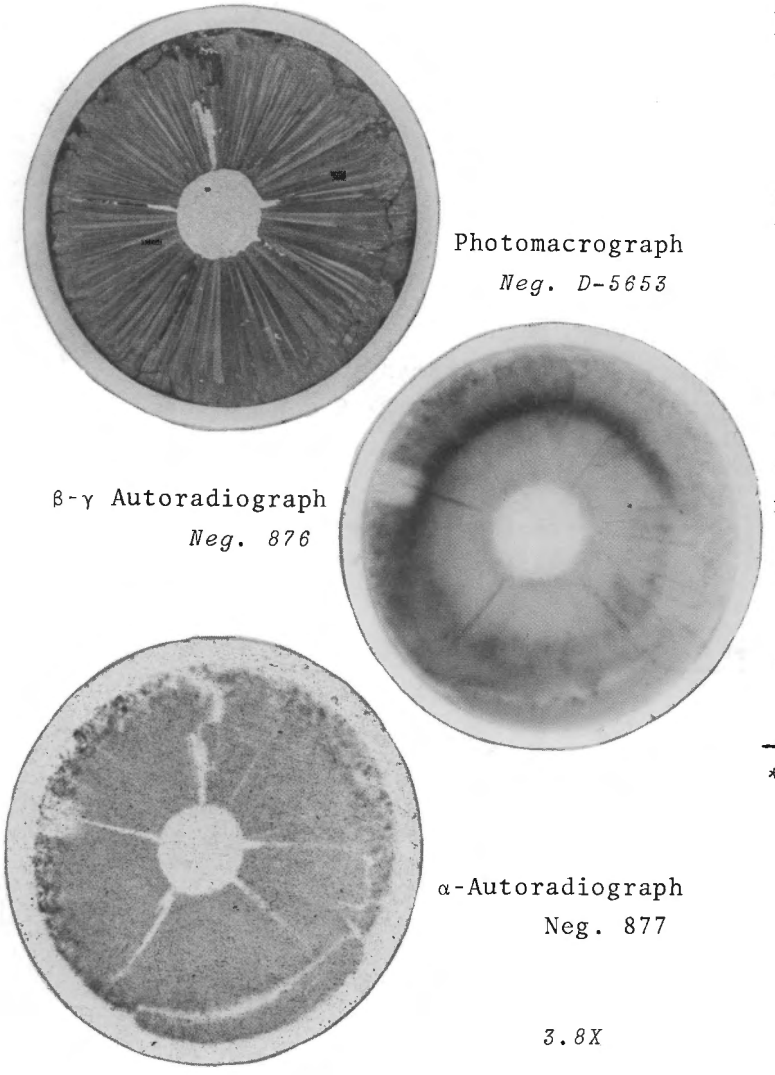

FIGURE 3. Transverse Section Through the Axial Midpoint of a Vibrationally Compacted UO_2–2 wt% PuO_2 PRTR Fuel Rod. The Rod Operated at a Maximum Power Generation of 20 kW/ft to a Burnup of 4950 MWd/tonne with Estimated Maximum Fuel Temperatures of 2600 to 2700 °C. Columnar Grain Growth Extends to 85% of the Radius.

compacted UO_2–2 wt% PuO_2 PRTR fuel rod (Figure 3) which was irradiated to a burnup of 4950 MWd/tonne at a maximum rod power of 20 kW/ft. In another instance, during the irradiation of a capsule containing UO_2–1.5 wt% PuO_2, the once-molten fuel structure, formed during an initially high but steadily decreasing rod power generation, was erased by time-temperature dependent solid state diffusion during long in-reactor exposure.[15]

In-reactor homogenization and solid-solution formation by UO_2 and PuO_2 interdiffusion starts in pneumatically impacted fuel at temperatures sufficient to cause sintering or equiaxed grain growth, and it occurs rapidly at the higher irradiation temperatures (Figure 4). The high degree of consolidation of the pneumatically impacted UO_2 and the small (-325 mesh) PuO_2 particles enhances the homogenizing process. Homogenization of the UO_2–PuO_2 fuel is apparent, on beta-gamma autoradiographs,* by

---

* *The beta-gamma autoradiographs described in this paper were made by exposing irradiated specimens to high resolution film plates which, after developing, indicate fission products. The alpha-autoradiographs[16] were made by exposing irradiated specimens to cellulose acetate, which, after etching in sodium hydroxide, indicate plutonium or alpha emitting isotopes associated with plutonium. Dark areas on both types of autoradiographs correspond to regions of high activity. Alpha energy analysis of microdrilled samples shows that ~32% of the total activity indicated by the alpha-autoradiograph is caused by alpha-energies normally associated with Cm^{242}. The remainder of the alpha activity is principally from plutonium isotopes and Am^{241}, although there was no significant amount of Am^{241} in the samples. Curium^{242} is associated with plutonium--originally included as enrichment material, plus that formed from U^{238}--because uranium decay chains modified by neutron reactions do not result in the formation of significant amounts of Curium. Curium^{242} is formed by the beta decay of Am^{242} which is formed by neutron capture in Am^{241}, a daughter product via beta decay of Pu^{241}.*

the lack of resolution of localized concentrations of fission products associated with discrete PuO_2 particles. Homogenization is indicated on the alpha-autoradiographs by the lack of resolution of the alpha emitters associated with discrete PuO_2 particles.

Melting in irradiated mixed-oxide fuel rods is evidenced by the formation of a well-defined region in the thermal center of the fuel—a region composed of a cellular or sometimes porous appearing subgrain structure. A band of pore-free high density grains, often characterized by a circumferential laminar appearing structure, is outside the well-defined porous fuel region. The remaining structure is similar to that described for the nonmolten condition.

MOLTEN FUEL OPERATION

Experience has shown that fuel melting occurs in 86% TD vibrationally compacted, pneumatically impacted UO_2–2 wt% PuO_2 at a linear rod power of 20 to 21 kW/ft under PRTR conditions. (The power generation required to produce the onset of melting is subject to refinement as more data are acquired.) This is equivalent[17]

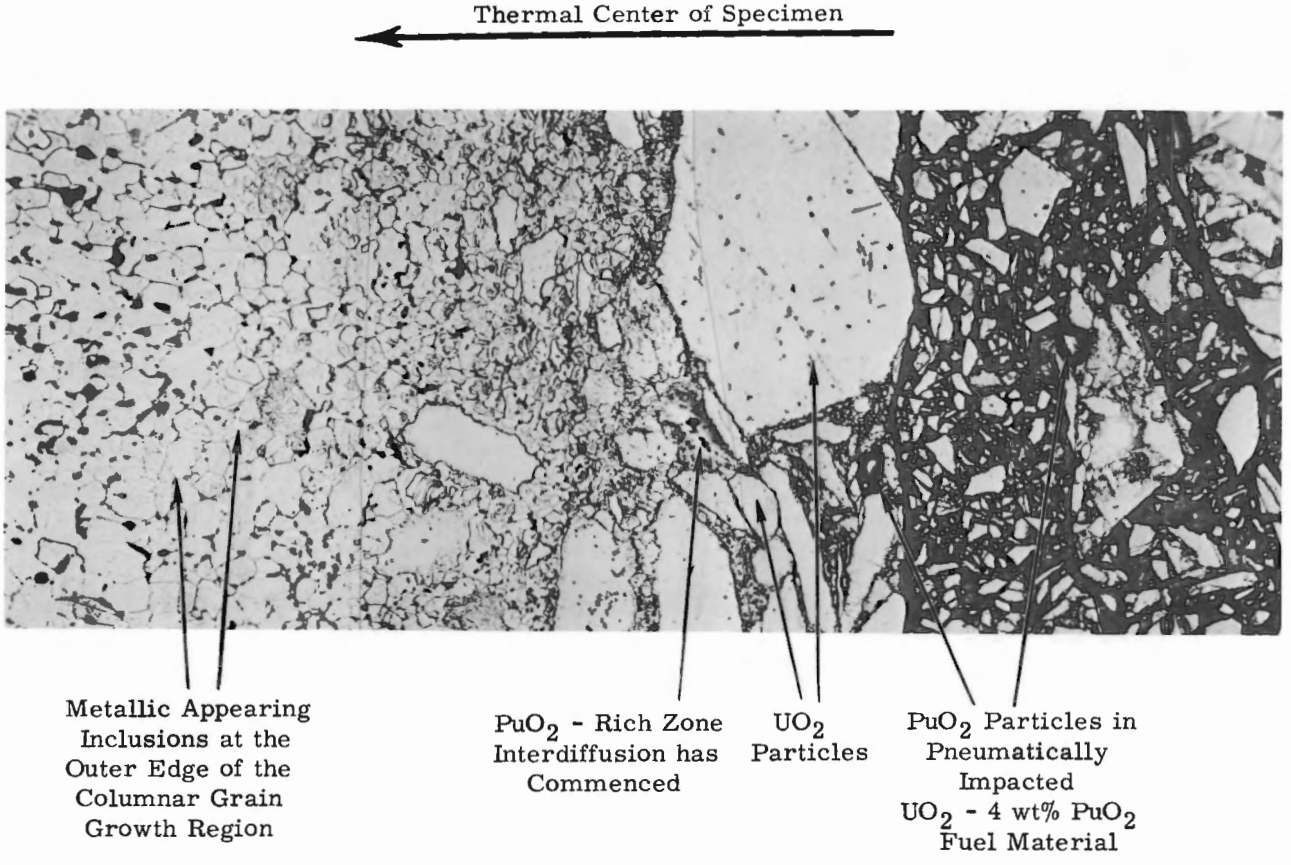

FIGURE 4. Photomicrograph of a Transverse Section from an Irradiated PRTR Fuel Rod Containing Vibrationally Compacted Pneumatically Impacted UO_2–4 wt% PuO_2 Fuel.

to an $\int_{T_s}^{T_m} K d\theta$ of 52 to 55 W/cm for UO_2–2 wt% PuO_2; or when compensating for the difference in self-shielding, it is comparable to an $\int_{T_s}^{T_m} K d\theta$ of 45 to 48 W/cm for similarly vibrationally compacted natural UO_2 where:

T_s = Temperature of fuel surface = 530 °C

T_m = Temperature of fuel melting = 2800 °C

K = Thermal conductivity of fuel

θ = Temperature.

This value is in good agreement with the value of 49 W/cm published by Lyons, et al.[18] The results show that the power to produce melting in vibrationally compacted fuels is ∿20% less than for sintered pellet fuel.

To minimize flux peaking in the end regions, prototype vibrationally compacted HPD fuel elements irradiated in PRTR were loaded with graded enrichment in the ends of the rods to prevent excessive fuel temperatures near the end caps. The graded enrichment in the bottom end regions consisted of a 1 cm thick depleted UO_2 pellet separating the end cap from a 3 cm length of UO_2–1 wt% PuO_2 fuel material adjacent to the UO_2–4 wt% PuO_2 fuel column.

Beta-gamma and alpha autoradiographs of a longitudinal section of the UO_2–1 wt% PuO_2 fuel region in the bottom end of a rod that had operated with fuel melting (maximum of 27 kW/ft) at the midplane indicated higher activities in the once-molten fuel region than in the surrounding non-molten fuel (Figure 5). Analyses of five microdrilled samples (Figure 5) show that the once-molten fuel contains 4 wt% PuO_2, while the surrounding non-molten fuel has 1 wt% PuO_2. The results of these analyses confirm the convective mixing of molten mixed-oxide in long fuel rods. This mixing tends to homogenize the molten fuel and average axial and radial burnup gradients and isotopic changes.

The beta-gamma autoradiograph (Figure 5) shows that the centrally located dark region coincides with the well-defined cellular structure on the photomosaic outlining the once-molten fuel region. The boundary of the centrally located dark or high plutonium-concentration region (shown by analysis to contain 4 wt% PuO_2) on the alpha-autoradiograph is more diffuse and extends beyond the well-defined cellular region on the photomosaic. In fact, the region of enriched plutonium extends beyond the surrounding high density band.

An interpretation of these analyses and observations is that the once-molten fuel region, at or near the time of shutdown, is represented by the well-defined cellular microstructure. The once-molten region is also delineated on the beta-gamma autoradiograph by the centrally located region of uniformly high fission product concentration. The boundary of the high plutonium-concentration region indicated on the alpha-autoradiograph does not necessarily correspond to the terminally molten fuel region. The alpha-autoradiograph shows that the initial molten fuel boundary possibly extended to the outer edge of the high density band. An increasing effective thermal

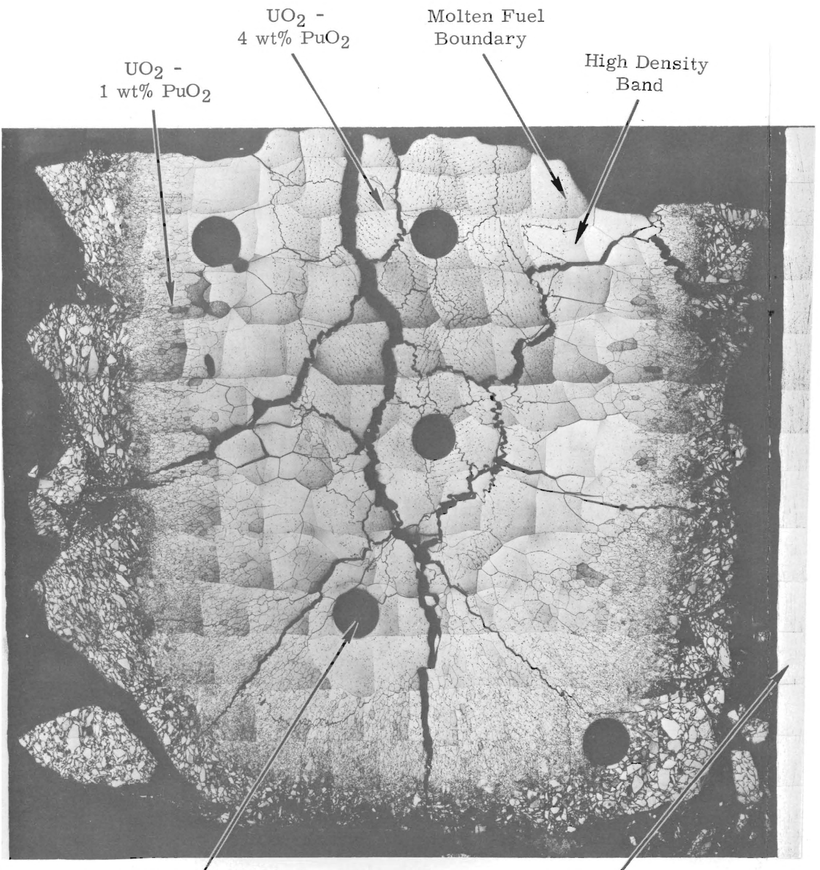

Photomacrograph (Mosaic)

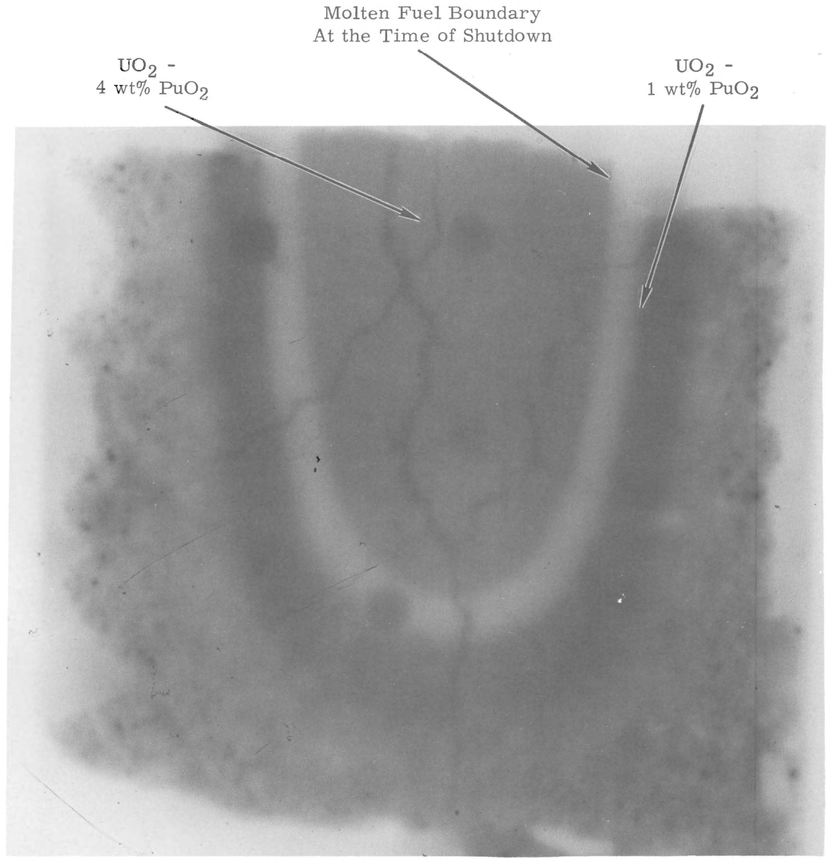

β-γ Autoradiograph

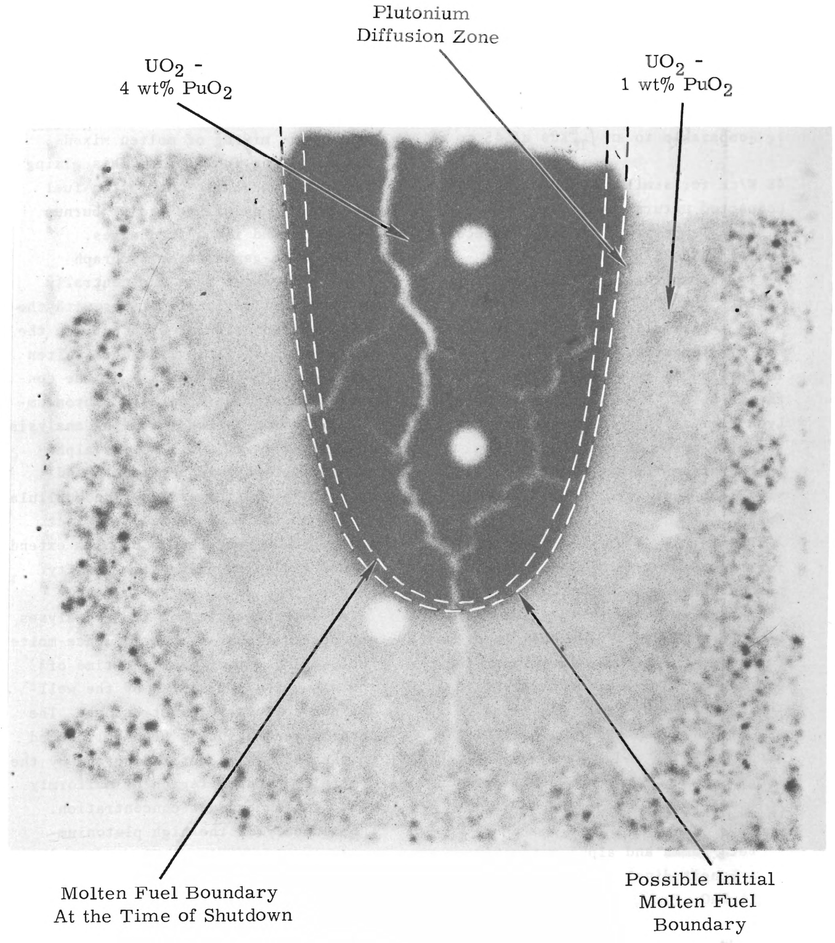

α-Autoradiograph

Neg. PNL0661684-5

13.4X

FIGURE 5. Longitudinal Section of the Bottom End Region of a Vibrationally Compacted UO_2-PuO_2 PRTR Fuel Rod. The Centrally Located Dark Region on the β-γ Autoradiograph Represents the Once-Molten Fuel Region at the Time of Shutdown and Contains 4 wt% PuO_2 from the Molten Fuel Column Above. The Dark Region on the α-Autoradiograph Extends Beyond the Final Molten Fuel Boundary Indicating a Receding Molten Boundary and/or Plutonium Diffusion into the UO_2-1 wt% PuO_2 Graded Enrichment Region.

conductivity, caused by in-reactor sintering of lower temperature fuel, would cause the molten boundary to recede, and a receding molten boundary is suggested by the laminar rings often observed in the high density band. The alpha-autoradiograph also indicates that plutonium diffused beyond the high density band into the nonmolten UO_2–1 wt% PuO_2 fuel region.

Postirradiation examination of many PRTR fuel rods that have operated with molten fuel shows that the diameter of the central void in the upper parts of rods is generally larger than it is below the midplane of the fuel column (Figure 6). In the upper regions, evidence of the once-molten fuel is generally found only on the inner surface of the central void, while in lower regions, one finds essentially no central void. This illustrates gravitational settling of molten fuel because the axial flux

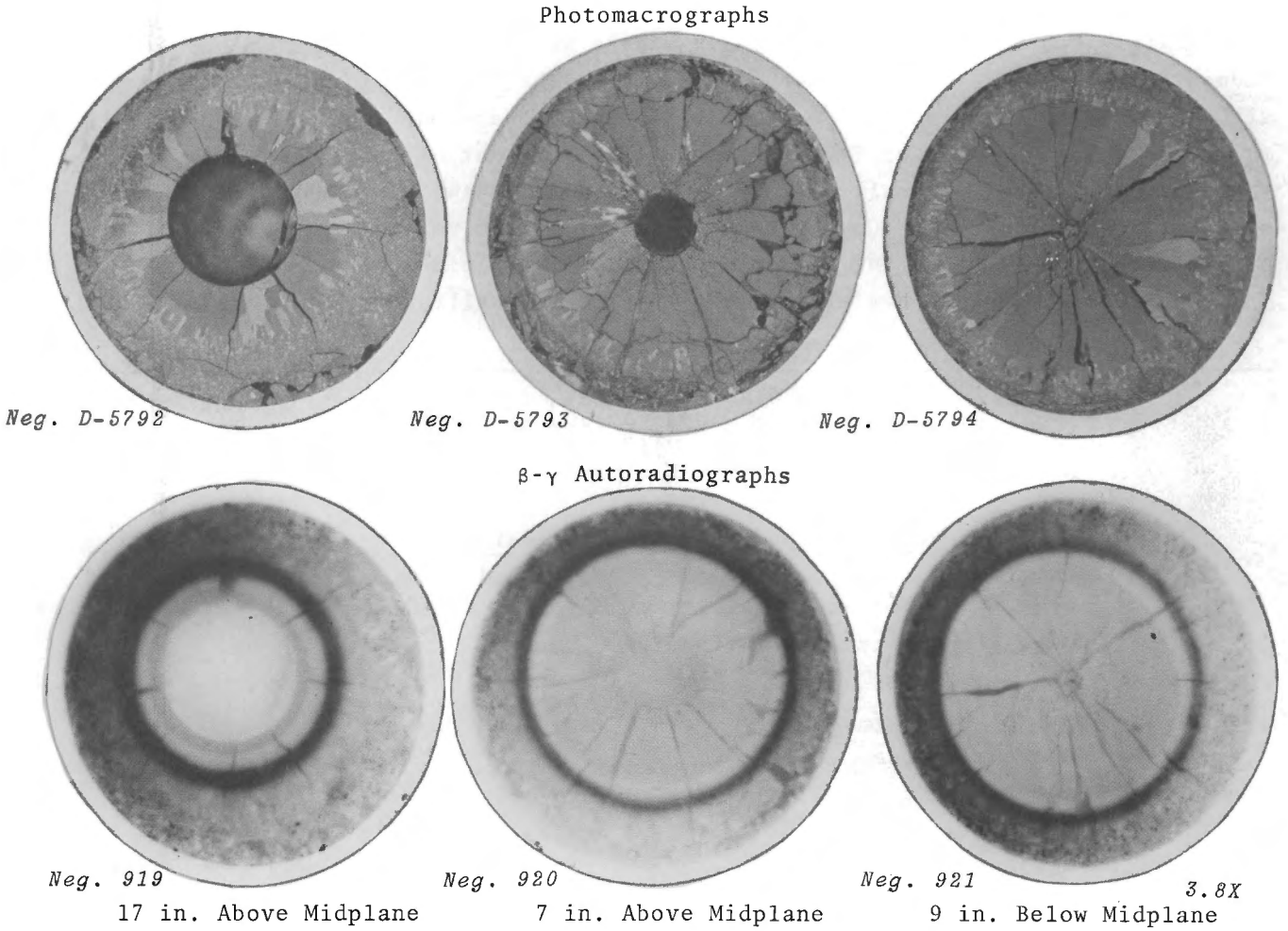

FIGURE 6. Transverse Sections at Different Planes Along the Length of a Vibrationally Compacted UO_2–4 wt% PuO_2 PRTR Fuel Rod (FB-55) that Operated with Significant (max. 63% of the radius) Fuel Melting.

distribution was essentially symmetrical about the midplane.

A PRTR 19 rod cluster fuel element (FE-6504) containing vibrationally compacted (86% TD) UO_2–4 wt% PuO_2 fuel was irradiated in the FERTF to an average burnup of 1040 MWd/tonne under molten core conditions (maximum rod power 27 kW/ft). The FERTF, positioned in the central tube of the PRTR, was surrounded by a flux trap and a ring of similar elements of equal burnup. No operating perturbations occurred to cause power variations within the 12 rod ring of the element. Hence, this ideal geometric situation permitted a comparison of the irradiation behavior of fuel rods that had experienced nominally the same irradiation history. Comparison of fuel structures formed in five rods from the 12 rod ring of this element shows a considerable variation in the structural characteristics of fuel irradiated under the same molten core conditions (Table I).

Fuel rod swelling was evidenced by an increased diameter (0.7% maximum) in the lower portion of two (FB-59 and FB-29) of the five rods examined (Table I). Examination of fuel structures formed during irradiation indicate that as much as 64% of the radius was molten in the swelled region of the rods. Fuel rod swelling can be expected under these conditions since there was not sufficient void volume within the fuel (excluding the plenum) to accommodate the volume expansion of this amount of molten material. The fuel rod swelling was probably caused by the volume expansion of molten fuel in the lower portion of the rod. Swelling occurred in this

TABLE I. Summary of Microstructural Features of Five Vibrationally Compacted UO_2–4 wt% PuO_2 Fuel Rods from the Twelve Rod Ring of a PRTR 19 Rod Cluster Element - (FE-6504)

Structure Boundary	% of Fuel Radius				
	Rod FB-06	Rod FB-83	Rod FB-59	Rod FB-55	Rod FB-29
Central Void, 17 in. above midplane	32	23	38	37	39
Central Void, 7 in. above midplane	26	76	8	17	21
Central Void, 9 in. below midplane	4	6	0	0	4
Fuel Melting, 17 in. above midplane	32	23	50	45	48
Fuel Melting, 7 in. above midplane	50	46	64	62	65
Fuel Melting, 9 in. below midplane	57	54	64	63	64

region because of a higher bulk fuel density resulting from axial fuel relocation or slumping. Axial fuel relocation is not unique with vibrationally compacted fuel since similar behavior has occurred in pellet containing fuel rods that have operated with fuel melting.[19] The other rods examined from this element operating under similar conditions did not show evidence of swelling.

DEFECT BEHAVIOR

The defect behavior of full-sized PRTR fuel elements operating under power reactor conditions has been investigated in the FERTF. Irradiations of intentionally defected PRTR fuel rods provided information on the relative fission product release rates from different types of defects. Generally, the defect behavior of ceramic packed-particle elements has been excellent. No appreciable fuel washout, fuel rod deformation, water-logging effects, or hydriding of the Zircaloy cladding was observed in any of the packed-particle fuel element defect tests. The only exception was the rupture of a deliberately defected rod operating with considerable fuel melting at the plane of the defect.[20] These tests included holes and longitudinal slit defects up to 6 in. long through the cladding of swage-compacted as well as vibrationally compacted PRTR fuel rods. A list of the defect tests performed in the FERTF is given in Table II, and the experimental results are discussed below.

FERTF TEST A:

A swaged UO_2 element (FE-1069), preirradiated to 1140 MWd/tonne, was defected with a 0.06 in. diam hole and irradiated in the loop at a maximum linear rod power of ∿7.3 kW/ft at the plane of the defect for ∿17 days; during which time, it was subjected to 6 pressurizations and 16 power cycles. Activity bursts during power level increases were ∿25 times greater than the steady state release rate. Repeated pressure and power cycling did not cause any perceptible fuel washout or water-logging. The zirconium hydride concentration of the cladding in the area of the defect increased from less than 100 ppm to ∿250 ppm.

FERTF TEST B:

A swage-compacted UO_2 element (FE-1039), preirradiated to 2440 MWd/tonne, was defected with a 0.62 in. long slit and irradiated at a maximum linear rod power of ∿7 kW/ft for 106 hr in the FERTF. During this time, the steady state activity release rates were ∿3.5 times greater than for the previous hole defect test. Power and pressure cycling did not cause any perceptible fuel washout, and no water-logging was evident.

FERTF TEST C:

The length of the longitudinal slit in FE-1039 was increased to 3.2 in. and the element was cycled through three startups and shutdowns during an additional 447 hr irradiation in the FERTF at a maximum linear rod power of ∿7 kW/ft. Steady state activity release rates were approximately the same as for the 0.62 in. long slit. There was no evidence of fuel element distortion, significant fuel release, or water-logging. Attempts to further

TABLE II. Coolant Activities from Defected Packed-Particle PRTR Elements Irradiated in the FERTF

Test No.	Element Type and No.	Cladding Defect	Maximum Rod Power (kW/ft)	Loop Activity, (cpm) Steady State GM (β,γ)	DN (delayed neutron)	Burst Activity GM (β,γ)	Type of Release
A.	Swaged UO_2 FE-1069	0.06 in. diam hole	7.3	8,000	4,000	220,000	Leaker[a]
B.	Swaged UO_2 FE-1039	0.62 in. long longitudinal slit	7.0	∿23,000[b]	∿13,000[b]	700,000	---
C.	Swaged UO_2 FE-1039	3.2 in. long longitudinal slit	7.0	23,000	13,000	100,000	Diffusion[c]
D.	Swaged UO_2 FE-1030	6.5 in. long longitudinal slit	6.1	68,000	38,000	150,000	Diffusion
E.	Vibrationally Compacted UO_2 FE-1067	3.0 in. long longitudinal slit	7.3	47,000	26,000	170,000	Diffusion
F.	Vibrationally Compacted UO_2 FE-1067	3.9 in. long longitudinal slit	7.3	60,000	31,000	---	Diffusion
G.	Vibrationally Compacted UO_2–2 wt% PuO_2 FE-6004	0.06 in. diam hole	24	80,000	4,000	660,000	Leaker
H.	Vibrationally Compacted UO_2–4 wt% PuO_2 FE-6504	0.06 in. diam hole	27	7.7×10^6[b]	1.6×10^5[b]	---	(Ruptured)

(a) *Poor communication between fuel and coolant - long delay time.*
(b) *Test was discontinued before stable form of release was established.*
(c) *Good communication between fuel and coolant - short delay time.*

increase the length of the slit were unsuccessful, and the irradiation of this element was terminated.

FERTF TEST D:

A swage-compacted preirradiated UO_2 element (FE-1030) was defected with a 6.5 in. long slit and irradiated for 16 days in the FERTF at a maximum linear rod power of ∿6.1 kW/ft. Postirradiation examination of the defected rod (preirradiated to 3270 MWd/tonne) showed no evidence of fuel washout, water-logging, or fuel rod swelling; the appearance of the slit was essentially the same as the preirradiated condition. In the center of the defect area, the zirconium hydride concentration in the cladding increased from less than 50 ppm to ∿100 ppm.

FERTF TEST E:

A vibrationally compacted UO_2 element (FE-1067) defected with a 3.0 in. long longitudinal slit was irradiated for 22 days in the FERTF at a maximum linear rod power of ∿7.3 kW/ft. Postirradiation examination of the defected rod (preirradiated to 1800 MWd/tonne) showed no evidence of fuel washout, water-logging, or significant fuel rod swelling. However, the slit appeared to have increased in width from 0.02 in. to ∿0.04 in. at the widest point. The steady state activity release rate from this element was midway between the release rates obtained for the 3.2 and 6.5 in. long slits in the swage-compacted UO_2 elements.

FERTF TEST F:

The length of the longitudinal slit in vibrationally compacted FE-1067 was increased to 3.9 in. and the element was irradiated for an additional 8 days in the FERTF at a maximum linear rod power of ∿7.3 kW/ft. (It was intended to increase it to 6.5 in.; however, postirradiation examination revealed that the slitting saw did not penetrate through the cladding for the intended distance.) The steady state activity release rate during this time was comparable to the release rate from the 6.5 in. long slit in swaged FE-1030 (FERTF Test D). These data indicate the fission product release rate for comparably sized defects is greater for vibrationally compacted elements than for swaged elements. Postirradiation examination again showed no evidence of appreciable fuel washout, water-logging, or additional fuel rod swelling.

FERTF TEST G:

A preirradiated, vibrationally compacted UO_2–2 wt% PuO_2 HPD fuel element (FE-6004), intentionally defected with a 0.06 in. diam hole through the cladding of one rod, was irradiated at a maximum linear rod power of ∿24 kW/ft at the plane of the defect. The rod operated successfully with fuel melting at the plane of the defect (Figure 7) for ∿60 hr until the test was terminated. Prior irradiation of this element in the nondefected condition at a maximum linear rod power of ∿19 kW/ft to a burnup of over 3500 MWd/tonne was sufficient to cause considerable in-reactor sintering of the fuel.

Burst type activity releases, characteristic of leaker defects, occurred during incremental power increases at the lower power levels. Incremental power increases at the higher levels produced less severe activity releases, but in all experiments during continued operation, the loop activity approached a steady-state value in an exponential manner. The steady-state gamma activity in the FERTF during irradiation of this element was ∿15 times greater than for any defected elements previously tested. However, the rod power of ∿24 kW/ft was ∿3 times greater than for any previous experiments. Activity bursts occurred when the reactor was shut down and also when the FERTF was depressurized.

There was essentially no change in the physical appearance of the defect, no dimensional changes in the rod, no significant fuel washout, and no metallographic evidence of increased hydride concentration in the cladding after irradiation in the FERTF (Figure 7). An observable effect of irradiation was a grey discoloration of the cladding downstream from the defect due to the evolution of material and/or gases from the defect.

The photomacrograph, beta-gamma autoradiograph, and alpha-autoradiograph (Figure 8) indicate that the symmetry of the fuel structure, fission product distribution, and alpha-emitter or plutonium distribution patterns were affected by the defect. The distribution of beta-gamma and alpha-emitters, as indicated on the autoradiographs, do not coincide except in the once-molten fuel region.

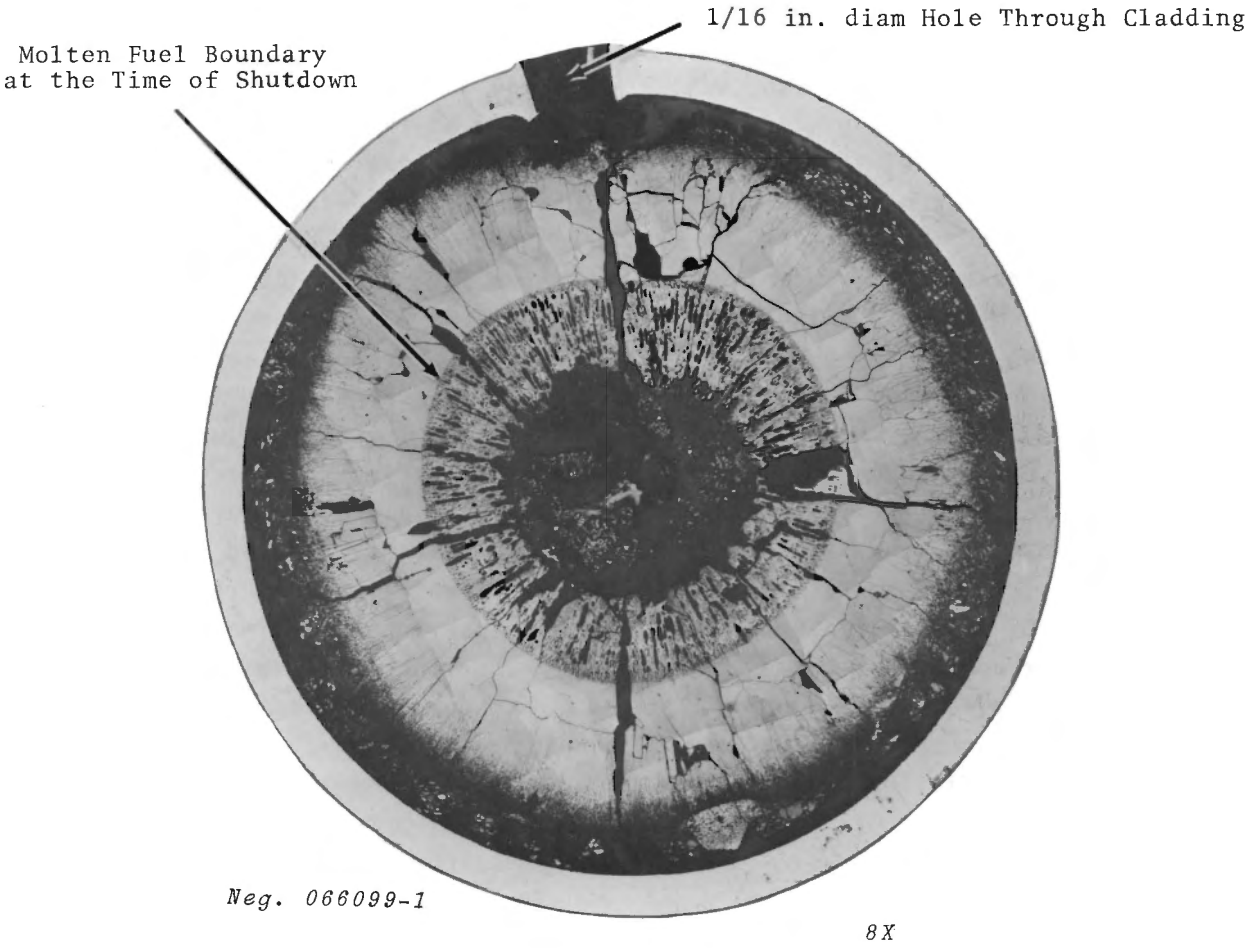

FIGURE 7. Photomosaic of a Transverse Section Through an Intentionally Defected UO_2–2 wt% PuO_2 PRTR Fuel Rod. Fuel Melting is Indicated to ~50% of the Radius.

Approximately the same amount of fuel melting was indicated in an adjacent nondefected rod also operating at a power generation of 24 kW/ft, (Figure 8). However, there was less porosity associated with the once-molten fuel region in the nondefected rod than in the adjacent defected rod, and the alpha-emitter (plutonium, distribution patterns) were different. The alpha-autoradiograph of the defected specimen indicates segregation of alpha-emitters from the once-molten fuel region, and migration into other regions of the specimen; whereas, the alpha-autoradiograph of the nondefected UO_2-PuO_2 fuel rod (Figure 8) shows no such segregation or migration.

FERTF TEST H:

An intentionally defected vibrationally compacted UO_2–4 wt% PuO_2 fuel rod and associated Zircaloy pressure tube ruptured while operating in the FERTF at a maximum rod power generation of 27 kW/ft with significant fuel melting.[20] Examination of the ruptured rod indicated that the cladding failed because of

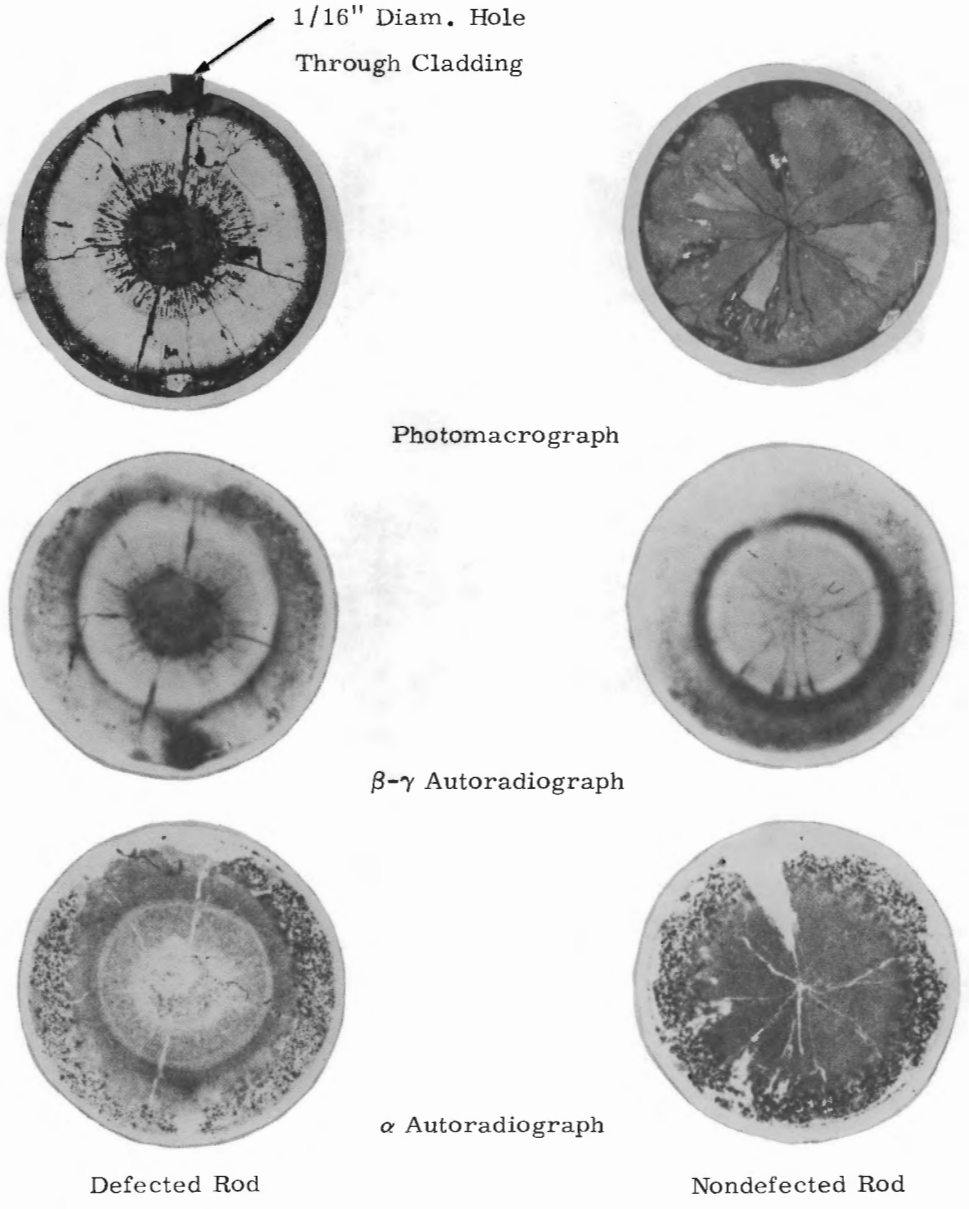

Neg. PNL0661684-1

FIGURE 8. Transverse Sections Through an Intentionally Defected and Nondefected Vibrationally Compacted UO_2–2 wt% PuO_2 PRTR Fuel Rod.

burnout or rapid hydriding caused by localized overheating. A sizeable piece of cladding (~3 in. long and almost 1/2 in. wide at the widest point) was missing from the area of the rod containing the defect (Figure 9). Approximately 700 grams of fuel material (39% of the total) were ejected from the rod, and fuel was completely missing over a distance of 5 in. in the vicinity of the rupture. The Zircaloy pressure tube was pene-

D-2778 0° D-2779 90° D-2776 180° D-2777 270°

Neg. PNL0661684-6 *0.8X*

FIGURE 9. Cladding Rupture in a Vibrationally Compacted UO_2–4 wt% PuO_2 PRTR Fuel Rod. Rupture Occurred in the Area of the Rod Previously Defected with a 1/16 in. diam Hole.

trated by a 1/2 in. diam hole adjacent to the rupture in the fuel rod. At the time of rupture the molten fuel in the rod was quickly and forcibly ejected from the fuel rod under pressure. This pressure was created between the inside of the fuel rod and the decreased FERTF coolant pressure when the pressure tube failed (Figure 10).

The precise mechanism by which failure occurred is not known. Post-irradiation examination indicates that the fuel in the ruptured rod operated at a significantly higher temperature than in adjacent nondefected rods operating at the same power generation. The unexpected large amount of fuel melting in the intentionally defected rod could have been caused by a decrease in the effective thermal conductivity of the fuel, a decrease in the melting temperature of the fuel, a slightly higher power generation due to venting

Neg. PNL0660164-6

16.8X

FIGURE 10. Transverse Section from the Upper Portion of the Ruptured Intentionally Defected PRTR Fuel Rod. The Molten UO_2–4 wt% PuO_2 Fuel was Rapidly Ejected from the Rod at the Time of Rupture.

fission gas poisons through the defect, or a combination of these effects. Although expansion of the unexpected large amount of molten fuel is considered to be the underlying cause of rupture, such behavior is not believed to be unique with vibrationally compacted UO_2-PuO_2 fuel.

Analysis of UO_2-PuO_2 fuel samples from the vicinity of the rupture shows that the O:U ratio increased from 2.01 before irradiation to ∿2.1 after irradiation. This analysis and other very recent data [21] suggest that in water vapor, UO_{2+x} might exist at higher temperatures than previously considered possible; also its formation can be very rapid. Increasing the O:U ratio from 2.00 to 2.15 reportedly decreases the heat rating required to produce fuel melting in UO_2 by ∿20%.[22] The decreased heat rating required to produce fuel melting is attributed principally to a lower melting temperature and reduced thermal conductivity. Increasing the O:U ratio from 2.00 to 2.15 decreases the melting point of UO_2 by as much as 400 °C.[23,24]

A direct comparison of the irradiation results of FERTF Test G and H is complicated because the irradiation conditions were not precisely the same. For instance, the defected rod that behaved satisfactorily did not have a fission gas plenum, and it operated at a maximum power generation of ∿24 kW/ft. The intentionally defected rod that ruptured contained a fission gas plenum; it operated at a maximum power generation of 27 kW/ft; and the coolant temperature was cycled during irradiation.

FISSION PRODUCT MIGRATION

Beta-gamma autoradiographs of irradiated mixed-oxide fuel specimens show that fission product migration commences at fuel temperatures sufficient to cause in-reactor sintering and grain growth.[6,15] Recently developed alpha-sensitive autoradiographic techniques[16] have shown that, under certain operating conditions, alpha emitter concentrations vary in irradiated mixed-oxide fuel specimens. Such variances indicate plutonium segregation from the liquid and migration in the solid.[6] The migration of fission products and plutonium during irradiation at high fuel temperatures could have a profound effect upon burnup analyses, reactivity, and fuel behavior.

Alpha autoradiography of UO_2-PuO_2 fuel specimens that operated with fuel melting suggests a difference in plutonium segregation and migration characteristics between defected and nondefected fuel rods. Activity distribution patterns in beta-gamma and alpha-autoradiographs of some irradiated UO_2-PuO_2 fuel specimens do not coincide. For example, in the beta-gamma and alpha-autoradiographs of the intentionally defected specimen (Figure 8), the only area that coincides is the once-molten fuel region near the center of the specimen. Other features of both types of autoradiographs correspond with structural changes in the irradiated specimen illustrated in the photomacrograph. The alpha-autoradiograph of the defected specimen (Figure 8) suggests segregation of plutonium from the

liquid phase, and migration in the solid phase during irradiation. However, as illustrated by the autoradiographs of a specimen from an adjacent nondefected UO_2-PuO_2 fuel rod (Figure 8), this effect has not been observed in every mixed-oxide specimen irradiated under molten fuel conditions. Since possible plutonium segregation effects have been most clearly indicated by alpha-autoradiographs of defected fuel specimens, a difference in the irradiation behavior (fission product migration and plutonium segregation) between defected and nondefected UO_2-PuO_2 fuel rods is suggested. This observation needs further evaluation.

The intentionally defected, vibrationally compacted UO_2–2 wt% PuO_2 PRTR fuel rod specimen (Figure 8) was drilled and radiochemically analyzed at selected locations.

Analytic results (Figure 11) show that Zr-Nb^{95}, Ce-Pr^{144}, and Sr^{90} migrate the least; whereas, Cs^{137} and Ru^{106} migrate the most. The Ru^{106} concentration can vary by more than an order of magnitude across the radius of a fuel rod, and a sharp increase in Ru^{106} concentration corresponds to the region of high activity on the beta-gamma autoradiograph at the inner edge of the small columnar grain growth region. The high activity region is characterized by a high concentration of metallic appearing inclusions (Figure 4). Similar appearing inclusions have been identified as metallic beta-uranium[25] in irradiated UO_2 and are probably associated with a high concentration of fission products and fission product (molybdenum, ruthenium) oxides.[26] Analytical results also indicate that the plutonium concentration does not vary appreciably across the radius of irradiated fuel specimens. There is no analytical evidence of plutonium segregation from the liquid or migration in the solid phase as suggested by the alpha-autoradiograph of the defected fuel rod (Figure 8).

FISSION GAS RELEASE

The amount of fission gas release has been determined for full-sized vibrationally compacted PRTR fuel rods containing pneumatically impacted UO_2-PuO_2 fuel. A plot of percent Xe + Kr release versus volumetric average fuel rod temperature ($T\bar{v}$)* for fuel rods with burnup ranging from 100 to 5000 MWd/tonne is given in Figure 12. The results show a maximum of 92% Xe + Kr release from fuel rods that operated with volumetric average fuel rod temperatures of ∿2200 °C produced by a maximum rod power of 27 kW/ft in PRTR. Fission

* *Volumetric average fuel temperatures are based on calculated temperature profiles within the fuel by using an estimated thermal conductivity of packed particle UO_2 as a function of temperature and the indicated thermal conductivity of UO_2 at 2800 °C as the thermal conductivity of molten fuel. The flux depression within UO_2-PuO_2 fuel rods is calculated with the THERMOS computer code. The volumetric average fuel temperature over the entire volume of the fuel rod is defined as:*

$$\bar{T}_v = \frac{Tv}{\phi/\bar{\phi}}$$

where $\bar{T}v$ = *Volumetric average fuel temperature within the fuel rod*

Tv = *Calculated volume weighted average fuel temperature at the maximum flux position*

ϕ = *Peak neutron flux*

$\bar{\phi}$ = *Average neutron flux along the length of the fuel rod.*

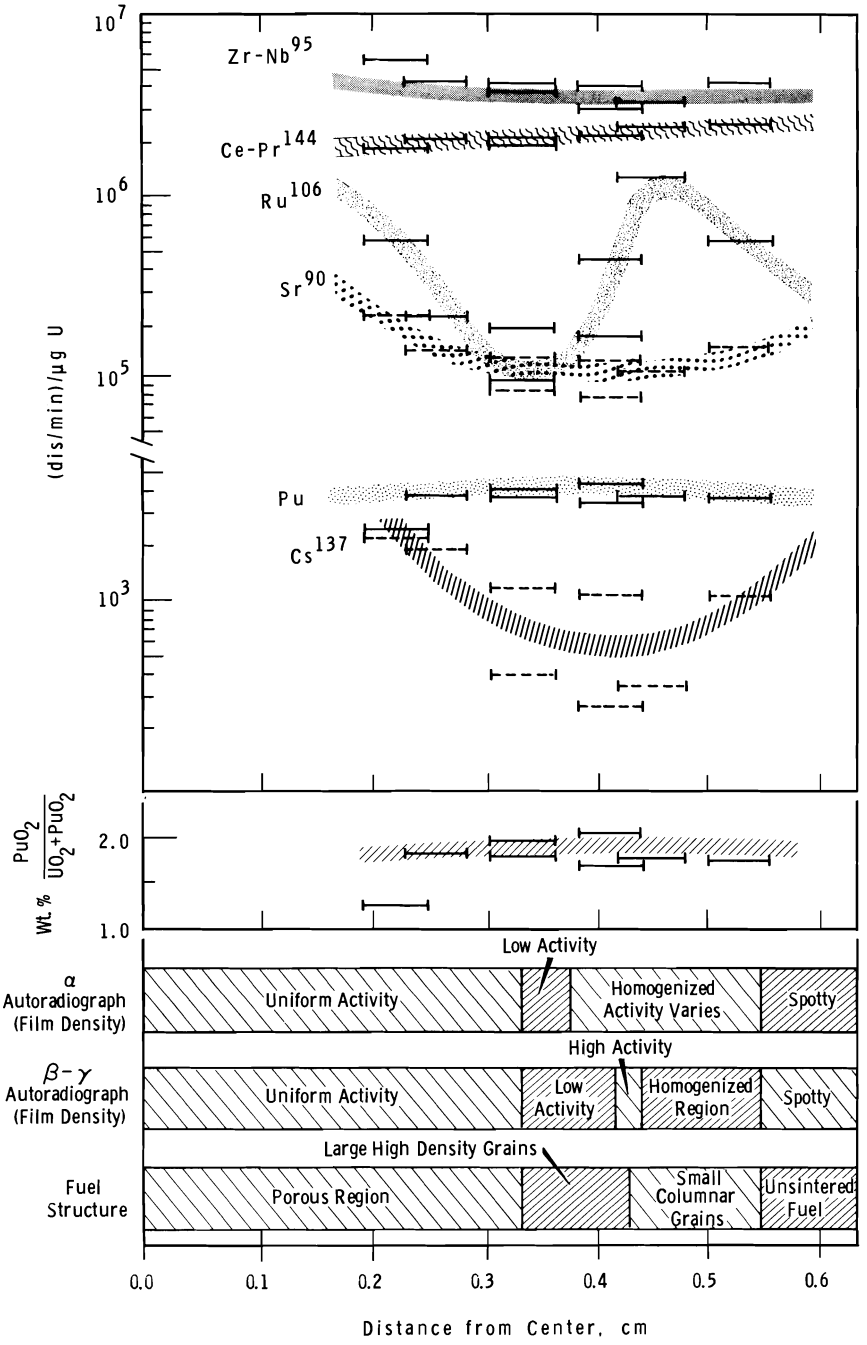

Neg. PNL0661473-1

FIGURE 11. Fission Product and Plutonium Distribution in the Intentionally Defected UO_2–2 wt% PuO_2 PRTR Fuel Specimen Shown in Figures 7 and 8.

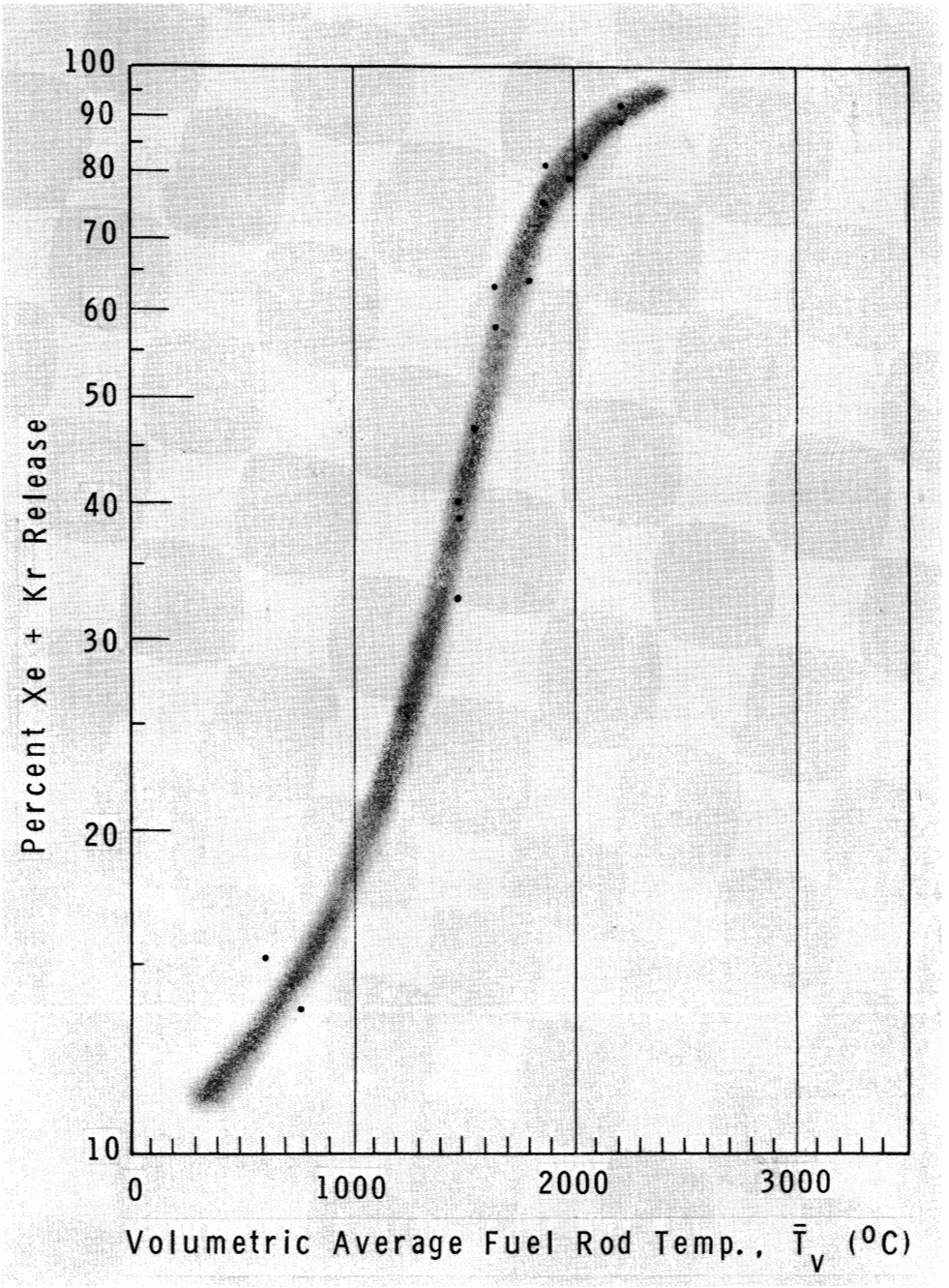

Neg. PNL0662928

FIGURE 12. Fission Gas Release as a Function of Volumetric Average Fuel Rod Temperature in Vibrationally Compacted UO_2-PuO_2 PRTR Fuel Rods.

gas release values are expected to increase with increasing burnup, particularly for the low fractional release values. However, the high fractional release values should not change appreciably with irradiation time because the rate of gas release from the high temperature fuel is more rapid.

Different rods from the same element, sampled in either the fuel or plenum region, yielded approximately the same quantity of gas, which indicated good communication along the entire length of the fuel rods and between plenum and fuel.

ACKNOWLEDGEMENT

The work described in this report represents the efforts of many individuals and organizations within Pacific Northwest Laboratory too numerous to mention individually. Their contributions are gratefully acknowledged.

REFERENCES

1. "Prospects for Plutonium Recycle," Nucleonics, vol. 24, no. 5, pp. 58-63. May, 1966.

2. F. W. Albaugh. "U. S. Program-Technology For Plutonium Fuels in Thermal Reactors," Panel on Use of Plutonium for Power Production. International Atomic Energy Agency, Vienna, Austria, December 7-11, 1964.

3. M. D. Freshley and Staff. "PRTR Fuel Element Experience," Trans. Am. Nucl. Soc., vol. 7, no. 2, p. 388-389. 1964.

4. N. G. Wittenbrock, P. C. Walkup, and J. K. Anderson. Plutonium Recycle Test Reactor, Final Safeguards Analysis, HW-61236. General Electric Company, Richland, Washington. October, 1959.

5. M. D. Freshley, F. E. Panisko, and R. E. Skavdahl. "Irradiation of UO_2-PuO_2 High Power Density Fuel Elements in PRTR," Trans. Am. Nucl. Soc., vol, 8, no. 2, p. 365-366. 1965.

6. M. D. Freshley, F. E. Panisko, and R. E. Skavdahl. "The Irradiation Behavior of UO_2-PuO_2 Fuels in PRTR," 1966 AIME Nuclear Metallurgy Symposium on High Temperature Nuclear Fuels, Delavan, Wisconsin, October 3-5, 1966.

7. F. G. Dawson. Program Analysis and Plans, Plutonium Utilization Program, FY-1967 Through 1970, BNWL-298. Pacific Northwest Laboratory, Richland, Washington. July, 1966.

8. J. R. Worden, W. L. Purcell, and L. C. Schmid. Physics Experiment, High Power Density Core of the PRTR, BNWL-221. Pacific Northwest Laboratory, Richland, Washington. January, 1966.

9. M. D. Freshley, R. E. Sharp, and R. E. Skavdahl. Plutonium Utilization Program: PRTR Irradiation Plans, BNWL-314. Pacific Northwest Laboratory, Richland, Washington. August, 1966.

10. P. C. Walkup. PRTR Fuel Element Rupture Test Facility, Capabilities and Project History, BNWL-40. Pacific Northwest Laboratory, Richland, Washington. March, 1965.

11. J. J. Hauth. Vibrational Compaction of Nuclear Fuels, BNWL-SA-579, Pacific Northwest Laboratory, Richland, Washington. March 1966.

12. D. W. Brite and C. A. Burgess. "High Energy Rate Pneumatically Impacted UO_2-PuO_2 Fuels," Trans. Am. Nucl. Soc., vol. 7, no. 2, p. 408. 1964.

13. R. E. Peterson. An Investigation of the Neutron Kinetics Problems Associated with Mixed Oxide Fuels, HW-81259. General Electric Company, Richland, Washington. July, 1966.

14. S. Goldsmith, M. D. Freshley, J. B. Burnham, and R. E. Skavdahl. "A Physically Mixed and Impacted UO_2-PuO_2 Fast Reactor Fuel," Trans. Am. Nucl. Soc., vol. 7, no. 2, p. 409. 1964.

15. R. E. Skavdahl, M. D. Freshley, W. J. Bailey, and S. Goldsmith. "Irradiation Properties of High Energy Rate Pneumatically Impacted UO_2-PuO_2 Fuels," The Third International Conference on Plutonium, London, England, November 1965.

16. J. H. Davies and R. W. Darmitzel. "Alpha Autoradiographic Technique for Irradiated Fuel," Nucleonics, vol. 23, no. 7, pp. 86-87. July, 1965.

17. J. A. L. Robertson. $\int K d\theta$ in Fuel Irradiations, CRFD-835. Atomic Energy of Canada Limited Chalk River, Ontario, April, 1959.

18. M. F. Lyons, D. H. Coplin, H. Hausner, B. Weidenbaum, and T. J. Pashos. UO_2 Powder and Pellet Thermal Conductivity During Irradiation, GEAP-5100-1. Atomic Power Equipment Dept., General Electric Co., San Jose, California. March, 1966.

19. M. F. Lyons, R. C. Nelson, T. J. Pashos, C. R. Wilson, and B. Weidenbaum. UO_2 Fuel Rod Operation With Gross Central Melting, GEAP-4264. Atomic Power Equipment Dept., General Electric Co., San Jose, California. October, 1963.

20. M. D. Freshley, R. G. Wheeler, J. M. Batch, and G. M. Hesson. Investigation of the Combined Failure of a Pressure Tube and Defected Fuel Rod in PRTR, BNWL-272. Pacific Northwest Laboratory, Richland, Washington. May 13, 1966.

21. R. C. Liimatainen, M. D. Freshley, and F. J. Testa. "Transient Irradiations of Vibrationally Compacted UO_2 Fuel in TREAT," Trans. Am. Nucl. Soc., vol. 9, no. 2, pp. 395-396. November, 1966.

22. J. A. Christensen, D. R. de Halas, and G. R. Horn. "Stoichiometry Effects in Molten Center Oxide Fuels-Oxygen Redistribution and Thermal Conductivity Effects," 1966 AIME Nuclear Metallurgy Symposium on High Temperature Nuclear Fuels, Delevan, Wisconsin, October 3-5, 1966.

23. J. A. Christensen. Irradiation Effects on UO_2 Melting, HW-69234. March, 1962.

24. J. L. Bates. "The Melting Points of Hypostoichiometric Uranium Dioxide," J. Am. Cer. Soc., vol. 49, no. 7, pp. 395-396. July, 1966.

25. J. L. Bates. Fission Product Distribution in Irradiated UO_2, BNWL-58. Pacific Northwest Laboratory, Richland, Washington, March, 1965.

26. B. T. Bradbury, J. T. Demant, P. M. Martin, and D. M. Poole. "Electron Probe Micro-Analysis of Irradiated UO_2," J. Nucl. Mat., vol. 17, p. 227. 1965.

DISTRIBUTION

Number of Copies

1 Alkem
7501 Leopoldshafen
Karlsruhe, Germany
W. Stoll

5 Argonne National Laboratory
C. H. Bean
J. H. Handwerk
J. H. Kittel
R. Macherey
J. F. Schumar

1 Associazione Euratom-CNEN Per I Reattori Veloci
Via Mazzini 2
Bologna, Italy
F. Pierantoni

2 Atomic Energy Commission, Richland
DRDT Site Representative
P. G. Holsted

5 Atomic Energy Commission, Washington
Division of Reactor Development
D. E. Erb
J. M. Morrisey
J. M. Simmons
W. R. Voigt
M. J. Whitman

3 Atomic Energy Research Establishment
Chemistry and Metallurgy Branch
Fuels Development Branch
Chalk River, Ontario, Canada
J. A. L. Robertson
O. J. C. Runnalls
A. S. Bain

4 Atomic Energy Research Establishment
United Kingdom Atomic Energy Authority
Harwell, Didcot, Berks, England
P. Murray (3)
L. E. Russell (1)

1 Atomics International
C. E. Weber

Number of Copies

2 Atomic Power Development Associates
119 First Street
Detroit 26, Michigan
W. H. Jens
A. A. Shoudy

4 Battelle Memorial Institute
D. L. Keller
S. W. Porembka (2)
W. F. Heenan (1)

1 Brookhaven National Laboratory
D. H. Gurinsky

1 Centre d'Etudes Nucleaires de Cadarache
Poite Postale No. 1
Saint-Paul-Lez-Durance, France
Dr. B. Defreyn

1 Combustion Engineering, Inc.
J. C. Tobin

277 Division of Technical Information Extension

3 Douglas United Nuclear, Inc.
T. W. Ambrose
L. E. Kusler
J. T. Stringer

1 European Atomic Energy Community
51-53 Rue Belliard (Euratom)
Brussels 4, Belgium
Pierre Kruys

1 General Electric Company, APD
Special Purpose Nuclear Systems Operation
P. O. Box 846
Pleasanton, California
J. E. Van Hoomissen

3 General Electric Company, Cincinnati
E. A. Aitken
W. Briskin
J. McGurty

Number of Copies

3 General Electric Company, Pleasanton
- L. P. Bupp
- E. A. Evans
- A. I. Kaznoff

5 General Electric Company, Richland
- R. L. Dickeman
- T. W. Evans
- M. Lewis
- C. H. Shaw
- E. A. Smith

7 General Electric Company, San Jose
- K. Cohen
- A. N. Holden
- F. J. Leitz
- M. F. Lyons
- T. J. Pashos
- R. E. Skavdahl
- B. Weidenbaum
- E. L. Zebroski

2 Isochem, Inc.
- H. H. Hopkins
- R. Y. Lyon

1 Kerr-McGee Indus. Inc.
Oklahoma City, Oklahoma
- Harold Lambertus

1 Knolls Atomic Power Laboratory
- W. K. Barney

5 Los Alamos Scientific Laboratory
- R. Baker
- M. Bowman
- H. Hessing
- D. MacMillan
- R. Spence

2 NASA Lewis Research Center
- A. F. Lietzke
- N. T. Saunders

4 Richland Operations Office
- C. L. Robinson
- R. K. Sharp (2)
- Technical Information Library

Number of Copies

1 Transuranium Institute (Euratom)
Karlsstrasse 42-44
Karlsruhe, Germany
- H. M. Mattys

4 Union Carbide Corporation (ORNL)
- R. M. Carroll
- J. L. Scott
- W. C. Thurber
- T. F. Connally

1 United Aircraft Corporation
Research Laboratory
East Hartford, Connecticut
- G. H. McLafferty

1 University of Arizona
Nuclear Engineering Department
Tucson, Arizona
- Monte V. Davis

1 University of California, Livermore
- Dr. James Hadley

1 University of Michigan
College of Engineering
Ann Arbor, Michigan
- W. Kerr

3 U. S. Atomic Energy Commission
Brussels, Belgium
- C. F. Schank

2 Westinghouse Bettis Atomic Power Laboratory
- J. Belle
- B. Lustman

4 Westinghouse Electric Corporation
- Robert Allio
- A. A. Bishop
- A. Boltax
- N. R. Nelson

1 Wright Air Development Center
AF Materials Laboratory
Wright-Patterson AFB,
Dayton, Ohio
- S. W. Bradstreet

214 Battelle-Northwest
- F. W. Albaugh
- H. J. Anderson
- R. J. Anicetti
- E. R. Astley

Number of Copies

Battelle-Northwest (contd)

J. A. Ayres
W. J. Bailey
R. J. Baker
R. E. Bardsley
J. M. Batch
J. L. Bates
A. L. Bement
T. K. Bierlein
C. H. Bloomster
D. W. Brite
C. A. Burgess
T. B. Burley
J. B. Burnham
S. H. Bush
J. J. Cadwell
T. D. Chikalla
J. A. Christensen
E. W. Christopherson
P. D. Cohn
R. E. Dahl
G. M. Dalen
J. L. Daniel
F. G. Dawson, Jr.
D. R. de Halas
R. F. Dickerson
R. L. Dillon
K. Drumheller
E. A. Eschbach
S. L. Fawcett
J. C. Fox
P. L. Farnsworth
J. R. Fishbaugher
M. C. Fraser
M. D. Freshley (100)
R. L. Gibby
S. Goldsmith
B. Griggs
R. L. Gulley
W. L. Hampson
H. E. Hanthorn
L. A. Hartcorn
H. Harty
B. R. Hayward
R. J. Hennig
G. M. Hesson
G. R. Horn
E. R. Irish
K. L. Junkins
J. P. Keenan
A. R. Keene
R. A. Kennedy
G. A. Last
D. C. Lehfeldt
W. R. Lewis

Number of Copies

R. J. Lobsinger
J. L. Maryott
C. E. McNeilly
L. G. Merker
M. K. Millhollen
J. E. Minor
D. E. Newby
R. E. Nightingale
L. J. Nitteberg
F. E. Panisko
P. J. Pankaskie
H. M. Parker
R. S. Paul
L. T. Pederson
L. A. Pember
A. M. Platt
R. H. Purcell
W. D. Richmond
W. E. Roake
R. K. Robinson
G. J. Rogers
L. C. Schmid
D. P. Shively
R. E. Sharp
R. C. Smith
R. I. Smith
E. A. Snajdr
D. H. Stewart
R. W. Stewart
K. R. Sump
W. H. Swift
H. A. Taylor
W. L. Thorne
G. L. Tingey
L. D. Turner
E. E. Voiland
P. C. Walkup
M. T. Walling
E. T. Weber
R. G. Wheeler
O. J. Wick
W. K. Winegardner
H. R. Wisely
N. G. Wittenbrock
F. W. Woodfield
J. R. Worden
D. C. Worlton
K. L. Young
H. H. Yoshikawa
F. R. Zaloudek
Technical Information Files (5)
Technical Publications(2)